

T. J. R. Hughes

Associate Professor of Mechanical Engineering,
Assoc. Mem. ASME

T. E. Tezduyar

Research Assistant.

Division of Applied Mechanics,
Stanford University,
Durand Building, Room 252,
Stanford, Calif. 94305

Finite Elements Based Upon Mindlin Plate Theory With Particular Reference to the Four-Node Bilinear Isoparametric Element

Concepts useful for the development of Mindlin plate elements are explored. Interpolation schemes and nodal patterns which are ideal according to the proposed criteria are found to be somewhat more complicated than desirable for practical applications. However, these ideas are found to be useful as starting points in the development of simpler elements. This is illustrated by the derivation of a new four-node bilinear quadrilateral which achieves good accuracy without ostensible defect.

1 Introduction

There has been considerable effort of late directed toward the development of improved plate and shell finite elements. Much of this effort has been focused upon theories which include transverse shear strain effects, for physical and computational reasons [22]. As a basis for the development of "displacement" plate elements of this type, the Mindlin theory [35] serves as the canonical starting point. Analogous, but generalized, theories may be used as the basis of shell element formulations. The "degeneration concept" is the terminology often applied to these ideas [1]. The literature on this topic, although mostly recent, has already become extensive. The interested reader may consult works among the following (incomplete) bibliography to familiarize himself with developments in this area: [6, 8, 9, 14-16, 19-25, 28, 29, 31, 37, 39-45, 49-52, 54, 56]. Although general improvement in element behavior is being sought, particular emphasis of late has been placed on reliability (i.e., making elements "fool proof") and simplicity. This latter requirement is an essential one in nonlinear analysis and especially in nonlinear transient analysis. Here, cost is the overriding consideration, and simple, inexpensive elements are actively sought after. Until fairly recently, there really was no plate or shell element which was sufficiently simple and inexpensive to be considered viable for large-scale nonlinear transient problems. However, the situation appears to be changing considerably as many efforts in the direction of simplicity have been performed (for a sampling of the literature on this topic, we may mention [3, 5, 7, 8, 17, 23-26, 28, 29, 31, 52, 54]). Progress is being made on many fronts, although a consensus favoring a particular approach is not yet in evi-

dence. Efforts of ours in this area have employed reduced and selective integration techniques (see e.g., [22-26]), a topic which has generated considerable literature in recent years.

Unfortunately, efforts to develop effective simple elements (e.g., 3-node triangles, 4-node quadrilaterals) often engender conceptual complexity. To make simple functions and nodal patterns work well seems to require the use of special procedures, or "tricks," depending on one's viewpoint. These encumbrances are quite puzzling to the nonspecialist and even create controversy among specialists.

One of the purposes of this paper, is to attempt to provide some explanation why special techniques are necessary for the development of simple, effective elements within the context of Mindlin plate theory. Based upon an idea due to MacNeal [31], we propose criteria for the development of Mindlin plate elements. Interpreted strictly, not allowing for reduced/selective integration or allied procedures, the interpolation schemes suggested involve different order polynomials for displacement and rotation, and consequently different nodal patterns. Thus it may be argued that "natural" elements, from the standpoint of the performance criterion, are neither natural nor convenient from implementational and practical standpoints. It is thus no wonder that elements of this type have apparently not been investigated heretofore. The traditionally used alternative of equal-order interpolation, if to be optimally effective, requires additional embellishments. This is acknowledged by a weakened version of the criterion, which accommodates the use of special techniques, such as reduced/selective integration. This form is, in fact, the one used by MacNeal [31].

These thoughts are, at first, somewhat disconcerting since they seem to imply that elements which should work well, within the standard Ritz-Galerkin framework, are not practically desirable. However, it is felt that there are lessons to be learned from these elements in that they may serve as conceptual starting points for elements which are simpler than their progenitors. We use this idea to generate a new four-node quadrilateral which employs bilinear iso-

Contributed by the Applied Mechanics Division for publication in the JOURNAL OF APPLIED MECHANICS.

Discussion on this paper should be addressed to the Editorial Department, ASME, United Engineering Center, 345 East 47th Street, New York, N. Y. 10017, and will be accepted until December 1, 1981. Readers who need more time to prepare a discussion should request an extension from the Editorial Department. Manuscript received by the Applied Mechanics Division, December, 1980; final revision, February, 1981.

parametric shape functions for all dependent variables. The element possesses correct rank and thus cures the spurious zero-energy mode problem which has beleaguered our previous endeavors on four-node plates [22, 26]. The new element turns out to have some features in common with MacNeal's QUAD4 [31], although it is felt that several advantages are accrued in the present formulation. These are mentioned as follows:

The development of the element for the general quadrilateral configuration is different from MacNeal's and appears to preclude some of the complications alluded to in [31]. In particular, no special local Cartesian system is necessary for effectuating good element behavior, or for achieving an invariant formulation.

In nonlinear analysis, the entire strain and stress tensors need to be calculated at each evaluation point. A shortcoming of what may be described as the classical selective integration procedure is that different components are calculated at different points, thus precluding straightforward generalization to nonlinear analysis. Recently, a generalization of selective integration has been developed which enables the pointwise definition of all strain, and consequently stress, components [18, 23]. The present element was developed within this format and thus may be straightforwardly generalized to the nonlinear case. This does not appear to be the case for QUAD4, in which a complicated variant on the selective integration theme is employed.

We have avoided the use of any *ad hoc* modification to attain special behavior under certain circumstances. Robinson [45] has criticized QUAD4 on this point because of its tunable aspect ratio parameter whose value is selected to give acceptable test results in certain single element test cases. Although we are sympathetic of efforts to improve high aspect ratio behavior, *ad hoc* techniques of this kind, based on linear test cases, become suspect in generalizing to nonlinear analysis, and even in linear cases, improvement in one situation may result in deterioration in another. (An example of this phenomenon is presented in Section 5.6, "The Twisted Ribbon.") Presently, aspect ratio deterioration is an ubiquitous, but poorly understood finite-element phenomenon.

Another area in which we have opted for simplicity, compared with QUAD4, is in the calculation of bending strains. MacNeal develops a special selective integration procedure to accurately represent certain cubic bending modes. (Herein we refer to these as "Kirchhoff modes," see Section 2.) MacNeal goes on to show that full cubic behavior is unattainable, despite the introduction of a further complication, namely, modification of stiffness parameters via so-called "residual bending flexibility." Since an order-of-accuracy improvement is not achieved, it is felt that the additional complications are unwarranted. Admittedly, the price is not high in linear analysis; however, in nonlinear analysis it is not at all clear what can even be done along these lines. Consequently, standard procedures are employed herein to calculate bending strains.

An outline of the remainder of the paper is given as follows. In Section 2, criteria for designing effective Mindlin plate elements are discussed. A link between function approximation (i.e., order of accuracy) and special techniques, such as reduced/selective integration, is incorporated in the criteria. Element interpolatory schemes and nodal patterns, suggested by these ideas, are presented.

Using one of the elements as a conceptual starting point, the new four-node bilinear quadrilateral plate is developed in Section 3. The only nonstandard feature of the development is the way transverse shear strains are interpolated, which is presented in detail in Section 3. In Section 4, implementational ideas are discussed. The special treatment of transverse shear strains manifests itself in the definition of the well-known "B-matrix" (i.e., strain-nodal displacement matrix) of finite-element theory. The modification falls within the framework presented in [18, 23]. In Section 4, numerical examples illustrate the good overall behavior of the element. Since it is now well known that plate/shell elements may behave well on one problem and pathologically on another, an extensive set of problem results is presented. The studies range from standard convergence tests to difficult problems, incorporating singular behavior, which tend to manifest element weaknesses. In addition, we consider a single-element test proposed

by Robinson [45] as a critical measure of the performance of a plate bending element. Conclusions are presented in Section 6.

It is felt that some of the ideas presented herein significantly contribute to the understanding of plate element design and behavior. Many new element possibilities arise in the presentation which will no doubt be the objects of future studies. Furthermore, it is hoped that analogous concepts will be useful in the study of related problem areas, such as continuum elements for incompressible, and nearly incompressible, behavior (see, e.g., [4, 12, 18, 19, 32-34, 36, 38, 48]).

The new four-node bilinear element developed herein is a decent performer. The overall accuracy level of the element appears to be good, without any ostensible defect, and this is accomplished while retaining simplicity. Nevertheless, it is not claimed to be a panacea. For example, its aspect ratio behavior on some problems is disappointing. Perhaps further improvement may be made here. On balance, however, it appears as good as any four-node element we have seen, perhaps better. It is a common practice for the developers of elements to see only the virtues of their own work, and only the sins of others, so we shall not belabor this point, leaving it for the reader to decide what is most appropriate for his/her circumstances.

2 Criteria for Designing Effective Mindlin Plate Elements

The first criterion which shed some light on the design of Mindlin plate elements was the method of constraint counting. This was employed in the investigations of Malkus and Hughes [34], Hughes, Cohen, and Haroun [22], and several studies of Hinton, Zienkiewicz, and colleagues (see, e.g., [42, 55]). Although helpful in predicting the performance of many plate elements, for some time it has been known that an overly pessimistic assessment may be obtained in certain situations. Recently, Spilker and Munir [49-51] have proposed a modified constraint counting measure, called a "rotational constraint index," which has achieved better correlation for the performance of hybrid plate elements.

The criterion advocated herein is based upon the ideas originally presented by MacNeal [31] and employed by Parisch [39]. Thin plate behavior is governed by the classical Poisson-Kirchhoff theory. In this limiting situation the face rotations become equal to the slopes of the transverse displacement field. Analytically, the rotations are no longer independent kinematic variables, but become the derivatives of the transverse displacement field. To assess the ability of Mindlin-type plate elements to correctly handle limiting thin-plate behavior, we shall examine the Mindlin elements with respect to the modes of deformation emanating from the classical theory.

To be more precise, let us define a *Kirchhoff mode* by the relation

$$\theta_{\alpha} = w_{,\alpha} \quad (1)$$

where w is a given transverse displacement; θ_{α} is the x_{α} -rotation, $\alpha = 1, 2$; and a comma is used to denote partial differentiation (e.g., $w_{,\alpha} = \partial w / \partial x_{\alpha}$).

A *Kirchhoff mode of order m* will be one in which w is taken to be a complete m th-order polynomial, $P_m(x_1, x_2)$. An example of a complete polynomial is the quadratic polynomial

$$P_2(x_1, x_2) = C_1 + C_2x_1 + C_3x_2 + C_4x_1^2 + C_5x_1x_2 + C_6x_2^2 \quad (2)$$

where the C 's are arbitrary coefficients.

Criterion 1. As a measure of the effectiveness of an element, we shall ask what order Kirchhoff mode the element is able to exactly interpolate. The higher the order, the greater the ability of the element to perform accurately in the thin-plate limit.

Criterion 2. A weakened version of the foregoing criterion, which accommodates reduced/selective integration and other procedures, asks for what order Kirchhoff mode is the strain energy calculated exactly. This is the form of the criterion employed by MacNeal [31] and Parisch [39]. Note that Criterion 1 implies Criterion 2.

Posing the criteria in terms of complete polynomials links up with order-of-accuracy concepts and may be useful in mathematical error analysis.

$w(\circ)$	quadratic	cubic	quartic
$\theta(\times)$	linear	quadratic	cubic
accuracy with respect to Kirchhoff modes	quadratic	cubic	quartic

Fig. 1 Beam elements derived from the Kirchhoff-mode criterion

Criterion 1 has the advantage that it suggests element interpolation schemes which may be effective. In this regard, it is immediately apparent that, according to Criterion 1, ideal interpolations may be devised by assuming w to be a polynomial one order higher than that assumed for the θ_α 's. Before considering some detailed examples of this type, it is worth remarking that schemes like this have apparently not been tried before and would be somewhat inconvenient from an implementational standpoint.

As a starting point, let us consider some one-dimensional beam-type examples. The lowest order possibility is quadratic displacement and linear rotation. (Note that linear displacement, constant rotation, is inadmissible since the rotation would necessarily be discontinuous, in violation of the continuity requirements of the governing theory.) The nodal pattern is illustrated in Fig. 1. This element achieves quadratic accuracy according to Criterion 1. The center displacement degree of freedom is inconvenient, however. An element of equivalent accuracy, in the sense of Criterion 2, which exclusively uses linear interpolations, may be devised by employing the reduced integration concept (one-point Gaussian quadrature need be used). This element was introduced in [26] and has led to the simplest effective two-dimensional shell formulations [14, 24, 25, 54]. In the linear constant coefficient case it can be shown to be identical to the quadratic displacement, linear rotation beam. (The center displacement degree of freedom may be statically condensed to yield an identical stiffness matrix [2].) Here we have a primitive illustration of the success of the reduced/selective integration concept, in that an element possessing a convenient interpolatory scheme may be made to behave like one possessing a higher-order, inconvenient scheme.

The next beam example consists of cubic interpolation for displacement and quadratic interpolation for rotation. The nodal pattern is illustrated in Fig. 1. Again, the internal degrees of freedom are inconvenient in practice. Static condensation leads to the usual element stiffness of structural theory (see, e.g., [10, p. 333]). An equivalent element may be obtained with quadratic interpolations for both w and θ , in conjunction with reduced two-point Gaussian quadrature. Again, static condensation of the internal degrees of freedom leads to the usual stiffness of structural theory [2]. Higher-order examples of this type may be constructed similarly.

Analogous two-dimensional interpolatory schemes may be devised for triangles. The triangular family illustrated in Fig. 2 appears unique among two-dimensional element families in that the functions which constitute the rotational interpolations are obtained exactly from the derivatives of displacement—no more, no less. This is unlike the situation for a somewhat analogous family of quadrilaterals in which Lagrange interpolations are used, the displacement being one order higher than the rotation (see Fig. 3).¹ For this family of elements, the

¹ In consideration of quadrilateral elements, for purposes of discussing Kirchhoff modal behavior, we shall assume a rectangular geometry.

w	quadratic	cubic	quartic
θ_α	linear	quadratic	cubic
accuracy with respect to Kirchhoff modes	quadratic	cubic	quartic

Fig. 2 Triangular plate elements derived from the Kirchhoff-mode criterion

w	biquadratic	bicubic	biquartic
θ_α	bilinear	biquadratic	bicubic
accuracy with respect to Kirchhoff modes	quadratic	cubic	quartic

Fig. 3 Quadrilateral Lagrange plate elements derived from the Kirchhoff-mode criterion

derivative of displacement contains more monomials than does the rotational interpolations. The classical Lagrange family of quadrilateral plate elements, in which identical interpolations are used for displacement and rotations (see Fig. 4), creates the opposite situation in that the rotational interpolation contains more monomials than does the derivative of displacement. That this situation is harmful has been suggested by Spilker and Munir [50]. Further research is required to determine the nature and extent of the problem when displacement and rotation fields fail to "match" according to the criteria. In any event, the triangular family of Fig. 2 appears canonical in this sense.

Of course, classical Lagrange-type interpolations, in which identical nodal patterns are employed for displacement and rotation (e.g., Fig. 4), are more easily implemented and applied than the new schemes suggested by the Kirchhoff modal criteria (i.e., Figs. 2 and 3). The behavior of Lagrangian elements has been shown to improve through use of the reduced/selective integration technique (unfortunately, so far at the expense of rank deficiency) [22, 42]. The excess rotational monomials are "filtered" by the lower-order quadrature resulting in higher-order behavior in the sense of Criterion 2. Thus we see again that convenient interpolations necessarily entail special procedures, such as reduced/selective integration and allied techniques, if they are to achieve optimal accuracy in practice. It has been argued that if high enough order interpolation (e.g., bicubic level) is used there is no need to employ reduced quadrature as adequate accuracy is

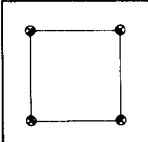
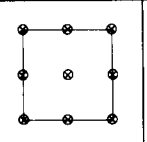
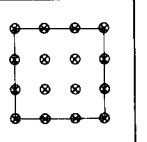
			
w, θ_a	bilinear	biquadratic	bicubic
accuracy with respect to Kirchhoff modes	linear	quadratic	cubic

Fig. 4 Classical Lagrange plate elements

achieved. The fact remains, however, that the behavior of such elements with full quadrature is suboptimal and may be further improved by the use of appropriate reduced/selective integration techniques.

In passing, we may note that the behavior of serendipity interpolatory schemes [53] is similar to Lagrange schemes with respect to Kirchhoff modal behavior. Specifically, classical schemes, in which the same interpolations are used for displacement and rotation, result in excess rotational monomials, whereas schemes in which displacement is interpolated one order higher than rotation possess excess monomials in the displacement-derivative field.

It is interesting to note that by using different interpolations for displacement and rotation, the possibility arises of devising "matched" interpolations for quadrilaterals. As an example of this phenomenon we may mention the combination of nine-node biquadratic Lagrange interpolation for displacement with eight-node serendipity interpolation for rotation. (This scheme has in fact been used as the starting point for the development of a discrete-Kirchhoff element by Irons [27].)

In summary, the ideal interpolations, with respect to the proposed criteria, are not the most desirable from the practical standpoint. In the sequel we shall attempt to use the idea of "optimal interpolation" (roughly speaking, one order higher for displacement than rotation) as a basis for the design of a practically appealing four-node quadrilateral element which simultaneously achieves simplicity and accuracy without engendering rank deficiency.

3 The Four-Node Bilinear Isoparametric Element

The present version of the four-node bilinear isoparametric element is based upon the concepts described in the previous section. The *conceptual* starting point is the straight-edged quadrilateral element in which transverse displacement is interpolated via nine-node Lagrange shape functions and rotations are interpolated via four-node bilinear shape functions (see Fig. 3). This element achieves quadratic accuracy with respect to Kirchhoff modes. The idea is to calculate the transverse shear strains in a special way independent of the midside and center node displacement degrees of freedom. In this way, the element stiffness senses only the corner node transverse displacement degrees of freedom and, consequently, four-node bilinear shape functions may be used in place of the nine-node Lagrange shape functions in formulating the element arrays. Examination of the interpolations reveals that the midpoints of the sides are locations at which the transverse shear strain components parallel to the sides are independent of the aforementioned nodal values. These four scalar values will be used to define the transverse shear strains. The details of the procedure follow.

Definition of Element Transverse Shear Strains. Geometric and kinematic data is defined in Fig. 5. Note that the direction vectors have unit length (e.g., $\|\mathbf{e}_{11}\| = 1$, etc.). Let w_a and θ_a denote the transverse displacement and rotation vector, respectively, associated with node a . Throughout, a subscript b will equal $a + 1$ modulo 4. That is

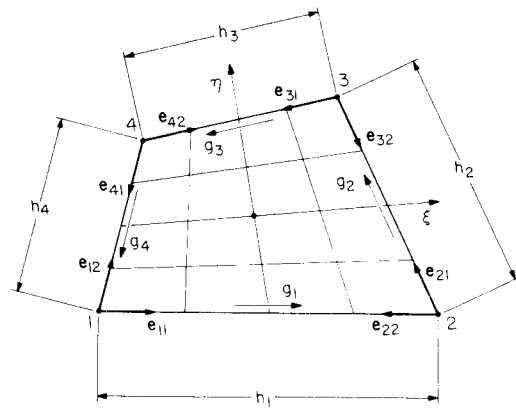


Fig. 5 Geometric and kinematic data for the four-node quadrilateral element

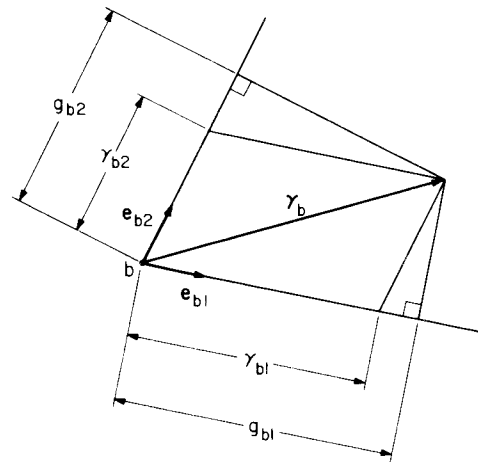


Fig. 6 Definition of nodal transverse shear strain vector

a	b
1	2
2	3
3	4
4	1

(3)

The definition of the element shear strains may be facilitated by the following steps:

1 For each element side define a shear strain component, located at the midpoint, in a direction parallel to the side, viz.,

$$g_a = (w_b - w_a)/h_a - \mathbf{e}_{a1} \cdot (\boldsymbol{\theta}_b + \boldsymbol{\theta}_a)/2. \quad (4)$$

2 For each node, define a shear strain vector (see Fig. 6 for a geometric interpretation of this process):

$$\boldsymbol{\gamma}_b = \gamma_{b1}\mathbf{e}_{b1} + \gamma_{b2}\mathbf{e}_{b2} \quad (5)$$

$$\gamma_{b2} = (1 - \alpha_b^2)^{-1}(g_{b2} - g_{b1}\alpha_b) \quad (6)$$

$$\gamma_{b1} = (1 - \alpha_b^2)^{-1}(g_{b1} - g_{b2}\alpha_b) \quad (7)$$

$$\alpha_b = \mathbf{e}_{b1} \cdot \mathbf{e}_{b2} \quad (8)$$

$$g_{b1} = g_b \quad (9)$$

$$g_{b2} = -g_a \quad (10)$$

3 Interpolate the nodal values by way of the bilinear shape functions (N_a 's).

$$\boldsymbol{\gamma} = \sum_{a=1}^4 N_a \boldsymbol{\gamma}_a \quad (11)$$

Remarks:

1 If the nodal transverse displacements and rotations are specified to consistently interpolate a constant transverse shear strain field, say $\bar{\gamma}$, then the preceding steps will result in $\gamma = \bar{\gamma}$. That is, constant transverse shear deformation modes are exactly representable in the general quadrilateral geometry.

2 In the rectangular configuration, the shear strains take on the following form (we assume the origin of coordinates coincides with the element center):

$$\gamma_1(x_2, x_2) = w_{,1}(0, 0) - \theta_1(0, 0) + x_2[w_{,12} - \theta_{1,2}(0, 0)] \quad (12)$$

$$\gamma_2(x_1, x_2) = w_{,2}(0, 0) - \theta_2(0, 0) + x_1[w_{,21} - \theta_{2,1}(0, 0)] \quad (13)$$

where $w_{,12} = w_{,21} = \text{constant}$. In this case the linear variations of γ_1 with x_2 and γ_2 with x_1 may be clearly seen. Note that there are four scalar transverse shear strain modes. (This may be concluded in general from the foregoing steps 1–3 which amount to an interpolation of the four scalar parameters $g_1, g_2, g_3,$ and g_4 .) These modes include the two constant transverse shear modes, and the “hourglass” and “in-plane twist” modes (see [22] for a discussion), thus enabling the element to achieve correct rank. In the rectangular configuration, the transverse shear strain variation is equivalent to the selective integration scheme of MacNeal [31]. The generalizations to quadrilateral configurations differ somewhat.

3 The “constraint index” (as defined in [34]) for the present element is -1 , which suggests failure in the thin-plate limit. As will be seen from the numerical examples, this is not the case, an illustration that the constraint index is sometimes overly pessimistic for plates.

4 To assess the effectiveness of the present element we employ the ideas of Section 2. Consider the rectangular configuration. It can be shown, with the aid of (12) and (13), that quadratic accuracy with respect to Kirchhoff modes is attained. This could be anticipated from the way the transverse shear strains were interpolated. The reduced/selective integration elements presented in [22, 26] effectively achieve the same end. However, they do not retain correct rank as does the present element.

5 Analogous procedures may be used to derive a three-node triangle employing linear shape functions. The conceptual starting point, in this case, is the triangle with quadratic w and linear θ_α 's (see Fig. 2). Again, quadratic accuracy with respect to Kirchhoff modes is achieved in the sense of Criterion 2. If effective in practice, this element would represent one of the simplest effective elements ever devised for bending applications.

4 Implementation

In this section we consider the implementation of Mindlin plate elements in which the same interpolatory patterns are used for displacement and rotations. This is general enough to encompass our new four-node element. It suffices in the present circumstances to consider the simpler case of a homogeneous, isotropic, linearly elastic plate of constant thickness t .

$$\mathbf{B}^b = [\mathbf{B}_1^b \mathbf{B}_2^b \dots \mathbf{B}_n^b] \quad (17)$$

$$\bar{\mathbf{B}}^s = [\bar{\mathbf{B}}_1^s \bar{\mathbf{B}}_2^s \dots \bar{\mathbf{B}}_n^s] \quad (18)$$

$$\mathbf{B}_a^b = \begin{bmatrix} 0 & N_{a,1} & 0 \\ 0 & 0 & N_{a,2} \\ 0 & N_{a,2} & N_{a,1} \end{bmatrix} \quad 1 \leq a \leq n. \quad (19)$$

The definition of $\bar{\mathbf{B}}_a^s$ is the essential ingredient in the development of an effective element. In the “normal” case, $\bar{\mathbf{B}}_a^s = \mathbf{B}_a^s$, which is defined by

$$\mathbf{B}_a^s = \begin{bmatrix} N_{a,1} & -N_a & 0 \\ N_{a,2} & 0 & -N_a \end{bmatrix} \quad 1 \leq a \leq n. \quad (20)$$

With this definition, some form of reduced/selective integration usually needs to be employed for success in the thin plate limit.

In the present formulation the reduced/selective-integration effect is accounted for directly in the definition of $\bar{\mathbf{B}}_a^s$ [18, 23]. For the transverse shear strain interpolations derived in the previous section, $\bar{\mathbf{B}}_a^s$ takes on the following form [recall the relation between subscripts a and b , see (3)]:

$$\bar{\mathbf{B}}_b^s = [\bar{\mathbf{B}}_{b1}^s \bar{\mathbf{B}}_{b2}^s \bar{\mathbf{B}}_{b3}^s] \quad 1 \leq b \leq 4 \quad (21)$$

$$\bar{\mathbf{B}}_{b1}^s = h_a^{-1} \mathbf{G}_a - h_b^{-1} \mathbf{G}_b \quad (22)$$

$$\bar{\mathbf{B}}_{b2}^s = (e_{b2}^1 \mathbf{G}_a - e_{b1}^1 \mathbf{G}_b) / 2 \quad (23)$$

$$\bar{\mathbf{B}}_{b3}^s = (e_{b2}^2 \mathbf{G}_a - e_{b1}^2 \mathbf{G}_b) / 2 \quad (24)$$

$$\mathbf{G}_a = (1 - \alpha_a^2)^{-1} N_a (\mathbf{e}_{a1} - \alpha_a \mathbf{e}_{a2}) - (1 - \alpha_b^2)^{-1} N_b (\mathbf{e}_{b2} - \alpha_b \mathbf{e}_{b1}) \quad (25)$$

$$\mathbf{e}_{b1} = \begin{Bmatrix} e_{b1}^1 \\ e_{b1}^2 \end{Bmatrix}, \text{ etc.} \quad (26)$$

The matrices \mathbf{D}^b and \mathbf{D}^s , for the isotropic, linearly elastic, constant thickness case, take on the following forms (respectively):

$$\mathbf{D}^b = \frac{t^3}{12} \begin{bmatrix} 2\mu + \bar{\lambda} & \bar{\lambda} & 0 \\ & 2\mu + \bar{\lambda} & 0 \\ \text{symm.} & & \mu \end{bmatrix} \quad (27)$$

and

$$\mathbf{D}^s = \kappa t \mu \begin{bmatrix} 1 & 0 \\ 0 & 1 \end{bmatrix} \quad (28)$$

where $\lambda = 2\lambda\mu/(\lambda + 2\mu)$, λ and μ are the Lamé parameters, and κ is a “shear correction factor,” which is taken to be $\frac{5}{6}$ throughout.

The external load vector, \mathbf{f}^e , is given by

$$\mathbf{f}^e = \{f_I^e\} \quad (29)$$

$$f_I^e = \begin{cases} \int_{A^e} N_a F dA + \int_{s^e \cap s_2} N_a Q ds, & I = 3a - 2, \quad 1 \leq a \leq n \\ - \int_{A^e} N_a C_\alpha dA - \int_{s^e \cap s_2} N_a M_\alpha ds, & I = 3a + \alpha - 2, \quad 1 \leq a \leq n, \quad \alpha = 1, 2 \end{cases} \quad (30)$$

Let A^e and s^e denote the area and boundary, respectively, of a typical element. Let N_1, N_2, \dots, N_n denote shape functions, where n is the number of element nodes.

The element stiffness matrix, \mathbf{k}^e , may be defined as follows:

$$\mathbf{k}^e = \mathbf{k}_b^e + \mathbf{k}_s^e \quad (14)$$

$$\mathbf{k}_b^e = \int_{A^e} \mathbf{B}^{bT} \mathbf{D}^b \mathbf{B}^b dA \quad \text{bending stiffness} \quad (15)$$

$$\mathbf{k}_s^e = \int_{A^e} \bar{\mathbf{B}}^{sT} \mathbf{D}^s \bar{\mathbf{B}}^s dA \quad \text{shear stiffness} \quad (16)$$

where F is the total applied transverse force per unit area, C_α is the total applied couple per unit area, Q is the applied shear force, M_α is the applied boundary moment, and s_2 is the portion of the plate boundary upon which forces and moments are prescribed.

The element stress resultants may be obtained from the following relations:

$$\begin{Bmatrix} m_{xx} \\ m_{yy} \\ m_{xy} \end{Bmatrix} = -\mathbf{D}^b \mathbf{B}^b \mathbf{d}^e \quad \text{bending moments} \quad (31)$$

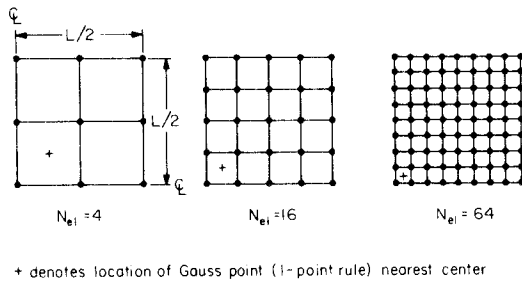


Fig. 7 Square plate meshes; due to symmetry, only one quadrant is discretized

$$\begin{Bmatrix} q_x \\ q_y \end{Bmatrix} = \mathbf{D}^s \mathbf{B}^s \mathbf{d}^e \quad \text{shear resultants} \quad (32)$$

where

$$\mathbf{d}^e = \{d_I^e\} \quad \text{element displacement vector} \quad (33)$$

$$d_I^e = \begin{cases} w_a, & I = 3a - 2, & 1 \leq a \leq n \\ \theta_{\alpha a}, & I = 3a + \alpha - 2, & 1 \leq a \leq n, \quad \alpha = 1, 2 \end{cases} \quad (34)$$

$$\theta_a = \begin{Bmatrix} \theta_{1a} \\ \theta_{2a} \end{Bmatrix} \quad (35)$$

Remark. Generalization of the formulation to fully nonlinear analysis is straightforward by way of the procedures described in [18, 23].

5 Numerical Examples

All calculations were performed at the California Institute of Technology Computer Center on an IBM 3032 computer in double precision (64 bits per floating point word). Unless otherwise specified, a Poisson's ratio of 0.3, Young's modulus of 10.92×10^5 , and geometric parameters $L = 10$ and $t = 0.1$ were used throughout.

In the context of Mindlin theory, two interpretations of the classical simply supported boundary condition are possible: SS_1 , in which only the transverse displacement is set to zero; and SS_2 , in which the transverse displacement and tangential rotation are set to zero. In applications to thin plates, SS_1 is generally preferable since it leads to convergent results when polygonal approximations of curved boundaries are employed. Nevertheless SS_2 corresponds to the simply supported condition of classical thin plate theory and may be safely employed for the analysis of polygonal, and in particular rectangular, plates. See [22] for a discussion of the treatment of simply supported boundary conditions and references to pertinent literature.

The following codes are used to denote the elements compared:

S1—This element employs 2×2 Gauss quadrature on the bending stiffness and one-point Gauss quadrature on the shear stiffness ("selective reduced integration"). It was originally proposed in [26] and has subsequently been studied extensively in [22] among other places. It possesses two spurious zero-energy modes [22, 26].

T1—This is the element developed herein; 2×2 Gauss quadrature it used on all terms. It possesses correct rank.

U1—This element employs one-point Gauss quadrature on all terms ("uniform reduced integration"). It was first proposed in [22] and studied therein. It possesses four spurious zero-energy modes.

In one case, the "twisted ribbon," we compare results with an element proposed by Robinson [45], dubbed LORA, and the MSC/NASTRAN element QUAD4 [31].

Despite the defects of S1 and U1 (i.e., spurious zero-energy modes) they behave well in many situations and are of interest because of their economy. With appropriate stabilization measures, such as so-called "hourglass" stiffness and viscosities, they hold significant potential in nonlinear analysis. See [11, 13, 30] for discussions of stabilization ideas employed in the continuum case.

In cases in which the dimensions enable the plate to be considered

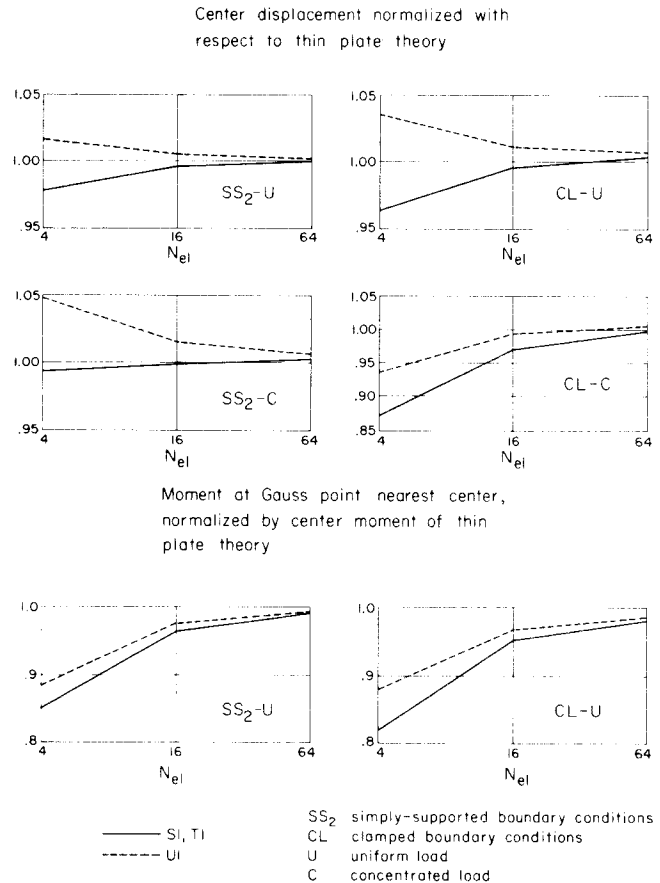


Fig. 8 Convergence study for thin square plate

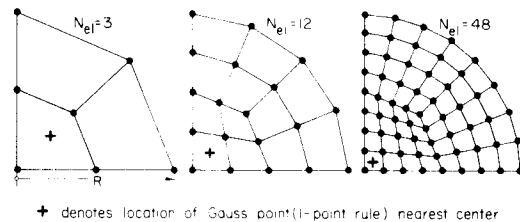


Fig. 9 Circular plate meshes; due to symmetry, only one quadrant is discretized

"thin," comparison is made with results of classical Poisson-Kirchhoff theory.

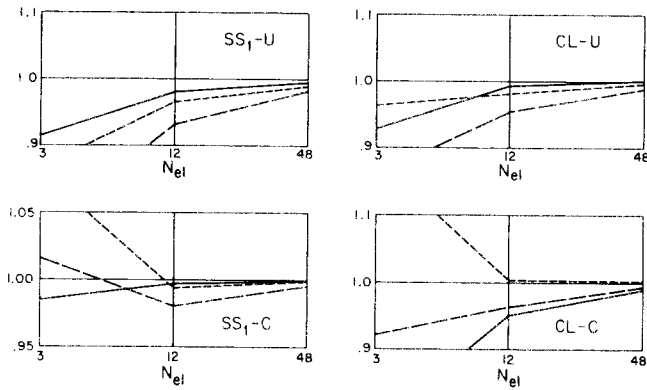
5.1 Thin Square Plate. This set of problems is perhaps the most common employed in testing plate element behavior. Meshes are depicted in Fig. 7 and results in Fig. 8. As may be seen, results for elements S1 and T1 are identical for plotting purposes. All elements perform well for this case.

5.2 Thin Circular Plate. These problems test the behavior of the elements in nonrectangular configurations. The radius $R = 5.0$. The meshes are shown in Fig. 9 and convergence results presented in Fig. 10. In this case, T1 is generally the best performer, although all elements perform well.

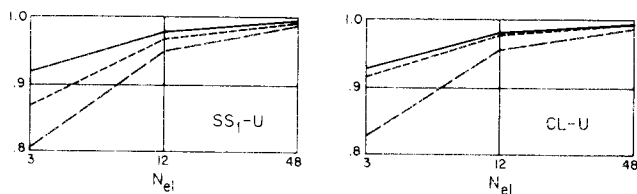
5.3 Thin Rectangular Plates. These problems test the response of the element to changes in planar aspect ratio. The meshes are shown in Figs. 11 and 12 and results are presented in Figs. 13 and 14. In these cases, as in the case of the square plate study, the differences between S1 and T1 are indiscernible on the scale of the plots.

As may be seen from Figs. 13 and 14, by far the worst displacement results are obtained for the clamped-boundary, concentrated-load

Center displacement normalized with respect to thin plate theory

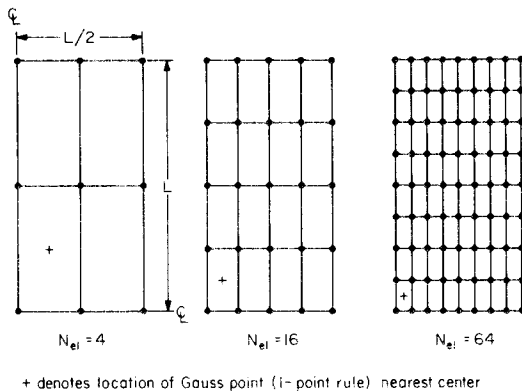


Moment at Gauss point nearest center, normalized by center moment of thin plate theory



--- S1
 --- T1
 --- UI
 SS1 simply-supported boundary conditions
 CL clamped boundary conditions
 U uniform load
 C concentrated load

Fig. 10 Convergence study for thin circular plate

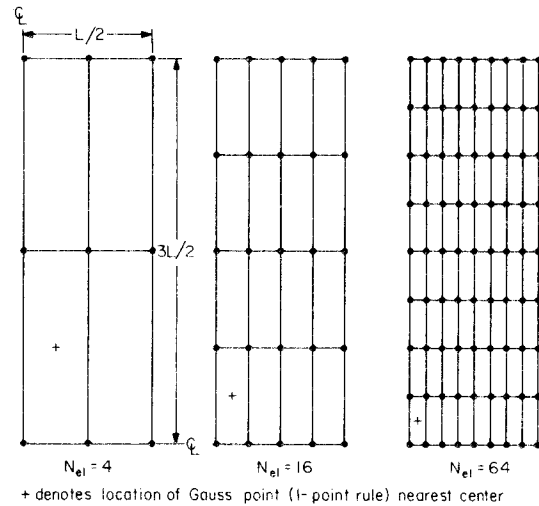


+ denotes location of Gauss point (1-point rule) nearest center

Fig. 11 Rectangular plate meshes (aspect ratio = 2); due to symmetry, only one quadrant is discretized

case. (This same pattern is in evidence for the square plate, see Fig. 8.) Robinson [45] has selected this case to compare S1 with an element he proposes, and some others, on crude meshes. Furthermore, some of the data he presents for S1 shows the error to be approximately twice the actual amount. Nevertheless it must be admitted that there is deterioration of accuracy with planar aspect ratio, a common, but not well-understood phenomenon for virtually all finite elements.

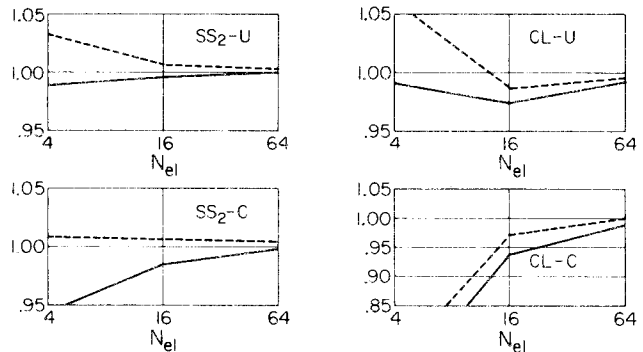
5.4 Thin Rhombic Plate. The configuration and mesh are shown in Fig. 15. The length parameter $\alpha = 100$. The plate is uniformly loaded and simply supported boundary conditions (SS1) are employed. This problem is a difficult one since there is a singularity at the obtuse vertex. The analytical solution reveals that the x_1 and x_2 bending moments have opposite signs in the vicinity of the obtuse vertex. Many thin plate elements yield pathological results for this



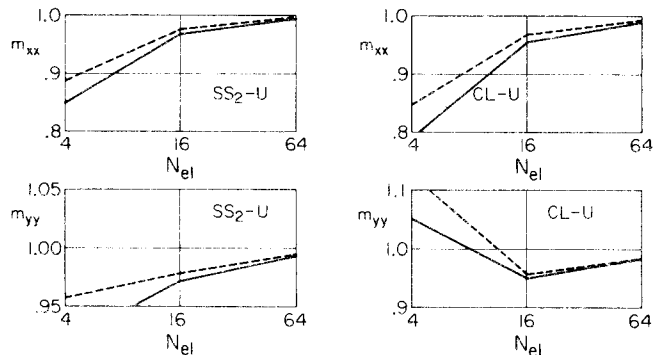
+ denotes location of Gauss point (1-point rule) nearest center

Fig. 12 Rectangular plate meshes (aspect ratio = 3); due to symmetry, only one quadrant is discretized

Center displacement normalized with respect to thin plate theory



Moment at Gauss point nearest center, normalized by center moment of thin plate theory



--- S1, T1
 --- UI
 SS2 simply-supported boundary conditions
 CL clamped boundary conditions
 U uniform load
 C concentrated load

Fig. 13 Convergence study for thin rectangular plate (aspect ratio = 2)

problem in that moments with the same sign are obtained (see [46, 47] for a discussion). Moment results are presented in Fig. 16. The general trend for each element is correct. However, the elements have a tendency to oscillate somewhat as may be seen. The worst oscillations are produced by U1. Considering that the mesh is not biased to favor the singularity, and that the problem is a numerically difficult one, the accuracy of the results obtained for S1 and U1 is considered to be fairly good.

5.5 Thick Circular Plate. This problem employs the same

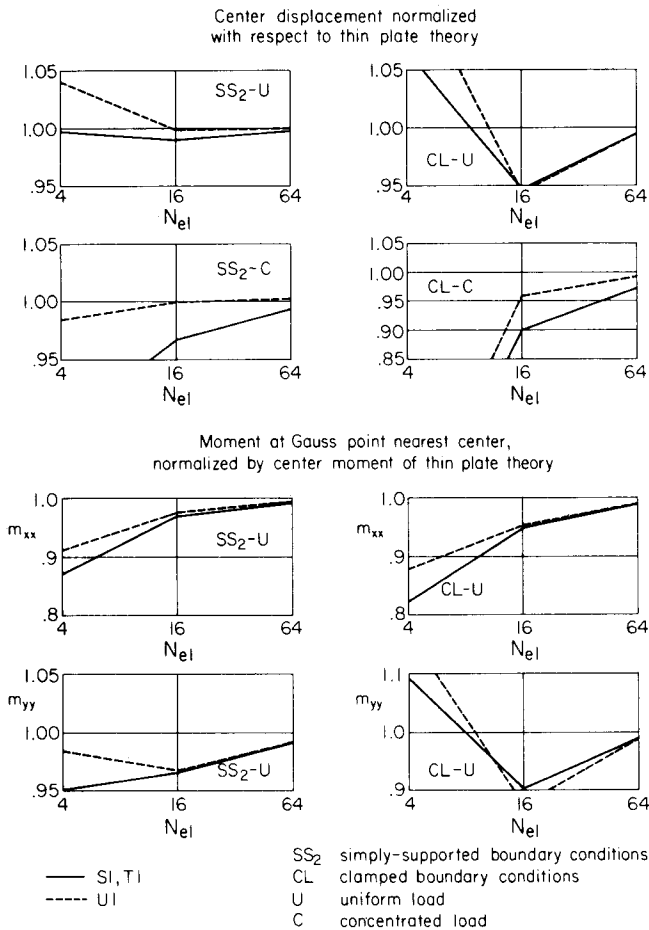


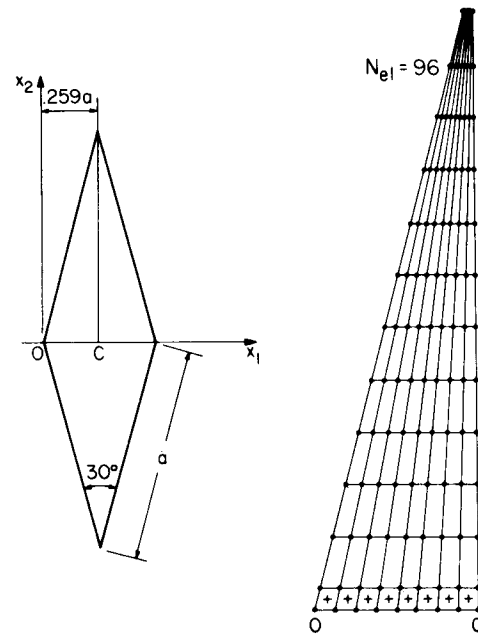
Fig. 14 Convergence study for thin rectangular plate (aspect ratio = 3)

48-element mesh as shown in Fig. 9, except the thickness is taken to be 2.0, and thus the plate may be considered "thick" ($R/t = 2.5$). It has been our experience that increasing thickness creates problems for rank-deficient elements [26]. An analytical solution obtained from Reissner's theory is used as a basis of comparison. The behavior under the load is singular and this gives rise to almost identical oscillatory patterns for elements S1 and U1 as may be seen in Fig. 17. On the other hand, element T1 produces very accurate results for this case.

5.6 Twisted Ribbon. Configurations, data and results for this problem are shown in Fig. 18. In each analysis, only one element is employed. Robinson [45] has proposed this as a critical single element test for plate bending elements. Comparisons are made with data presented in [45] for Robinson's element, LORA, and MacNeal's QUAD4 [31].

For Cases A and C (fully fixed boundary), comparison is made with respect to a benchmark analysis, reported upon in [45], involving sixteen high-precision elements. As may be seen, the results for our new element T1 are superior to the results for both LORA and QUAD4. Furthermore, no deterioration with increasing aspect ratio is detected. For this case, elements S1 and U1 exhibit pathological behavior due to rank deficiency (not shown).

It is interesting to note that Robinson [45], in advocating the use of LORA, has particularly emphasized its good behavior with respect to aspect ratio. Clearly, however, there is significant and inexplicable deterioration of LORA in Case B. Special emphasis has also been given to aspect ratio behavior by MacNeal [31] in the development of QUAD4. The technique employed is *ad hoc* and employs an adjustable parameter. Although improvement is noted in some situations, deterioration is encountered in others, as may be concluded from the comparison of T1 and QUAD4 in this example.



+ denotes Gauss points (1-point rule) nearest $x_2 = 0$

Fig. 15 Rhombic plate mesh; due to symmetry, only one quadrant is discretized

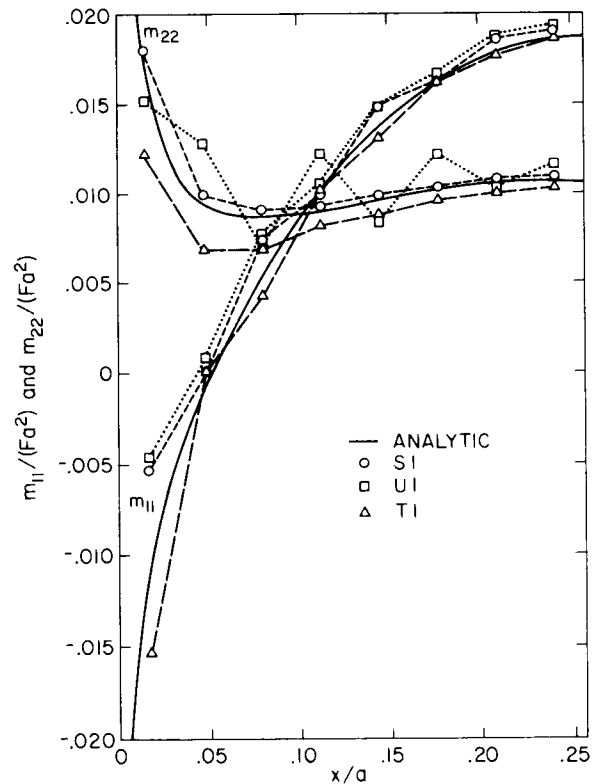


Fig. 16 Bending moments for rhombic plate

If only half the domain is modeled, and antisymmetrical boundary conditions are enforced (Cases C and D), the exact solution is one of pure twist. For these cases, S1 and T1 yield exact solutions, whereas U1 still behaves pathologically (not shown).

6 Conclusions

In this paper a new conceptual framework has been established for

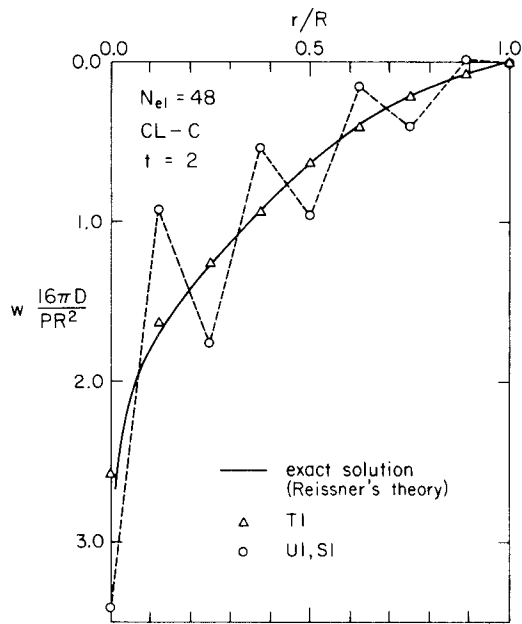


Fig. 17 Displacement results for thick circular plate

the development of plate elements based on Mindlin theory. The interpolatory patterns suggested have not been studied heretofore, but are somewhat more complicated than practical requirements presently dictate. It is proposed, however, that the ideas are useful in the development of more appealing elements, and this is illustrated by the development of a new four-node quadrilateral element employing bilinear isoparametric interpolation for all dependent variables. The element represents an improvement over past efforts of ours in that no spurious zero-energy modes are present. Simplicity is retained in the formulation and the element is shown to behave well on a variety of plate problems. The formulation enables straightfor-

ward generalization to nonlinear analysis, and appears to have some advantages over competing elements.

Considerable further work remains to be done in exploring the behavior of some of the new elements proposed herein. In addition, serious studies of aspect ratio effects and transverse shear resultants would be very helpful in improving the understanding of element response. Finally, the rigorous mathematical convergence analysis of elements of the type considered in this work, which is a delicate matter judging from related studies [38, 48], needs to be assiduously pursued to put matters on a sound footing.

Acknowledgment

We wish to thank the following individuals and organizations for providing support for our research: J. Crawford and T. Shugar of the Civil Engineering Laboratory, Port Hueneme, Calif., the National Science Foundation, and J. Carey of the Electric Power Research Institute, Palo Alto, Calif.

References

- 1 Ahmad, S., Irons, B. M., and Zienkiewicz, O. C., "Analysis of Thick and Thin Shell Structures by Curved Finite Elements," *International Journal for Numerical Methods in Engineering*, Vol. 2, 1970, pp 419-451.
- 2 Allik, H., Private Communication, 1976.
- 3 Argyris, J. H., and Dunne, P. C., "Postbuckling, Finite-Element Analysis of Circular Cylinders Under End Load," Report No. 224, Institut für Statik und Dynamik der Luft-und Raumfahrtkonstruktionen, University of Stuttgart, Germany, 1977.
- 4 Argyris, J. H., et al., "Large Natural Strains and Some Special Difficulties Due to Nonlinearity and Incompressibility in Finite Elements," *Computer Methods in Applied Mechanics and Engineering*, Vol. 4, 1974, pp. 219-278.
- 5 Argyris, J. H., et al., "A Simple Triangular Facet Shell Element With Applications to Linear and Nonlinear Equilibrium and Elastic Stability Problems," *Computer Methods in Applied Mechanics and Engineering*, Vol. 10, No. 3, Mar. 1977, pp. 371-403; Vol. 11, No. 1, Apr. 1977, pp. 97-131.
- 6 Bathe, K. J., and Bolourchi, S., "A Geometric and Material Nonlinear Plate and Shell Element," *Computers and Structures*, to appear.
- 7 Batoz, J. L., Bathe, K. J., and Ho, L. W., "A Search for the Optimum Three-Node Triangular Plate Bending Element," Report 82448-8, Massachusetts Institute of Technology, Cambridge, Mass., Dec. 1978.
- 8 Berkovic, M., "Thin Shell Isoparametric Elements," *Proceedings of the Second World Congress on Finite Element Methods*, Bournemouth, Dorset, England, Oct. 1978.
- 9 Bolourchi, S., "On Finite-Element Analysis of General Shell Structures,"

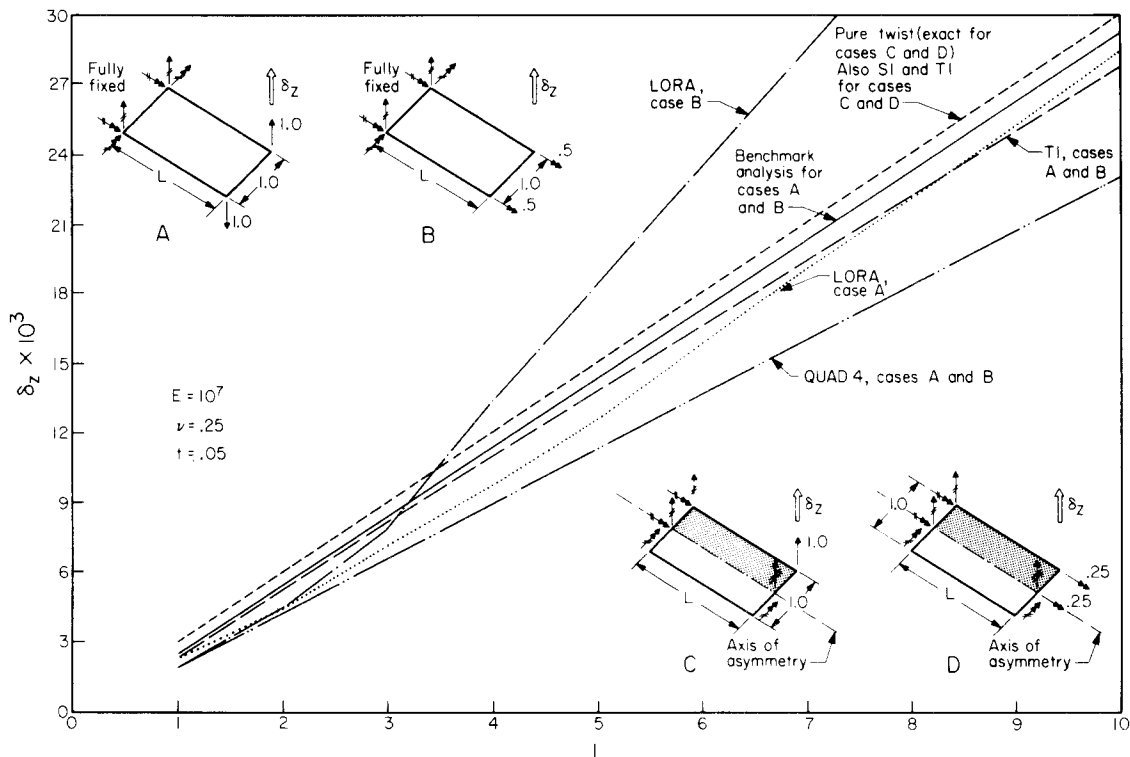


Fig. 18 Displacement results for the twisted ribbon; one element used in all cases

PhD Dissertation, Massachusetts Institute of Technology, Cambridge, Mass., May 1979.

10 Cook, R. D., *Concepts and Applications of Finite-Element Analysis*, John Wiley, New York, 1974.

11 Flanagan, D. P., and Belytschko, T., "A Uniform Strain Hexahedron and Quadrilateral With Orthogonal Hour Glass Control," preprint.

12 Fried, I., "Finite-Element Analysis of Incompressible Material by Residual Energy Balancing," *International Journal of Solids and Structures*, Vol. 10, 1974, pp. 993-1002.

13 Giroux, E. D., "HEMP User's Manual," University of California, Lawrence Livermore Laboratory, Report UCRL-51079, 1973.

14 Goudreau, G. L., "A Computer Module for One Step Dynamic Response of an Axisymmetric Plane Linear Elastic Thin Shell," Lawrence Livermore Laboratory Report No. UCID-17730, Feb. 1978.

15 Hinton, E., and Bicanic, N., "A Comparison of Lagrangian and Serendipity Mindlin Plate Elements for Free Vibration Analysis," *Computers and Structures*, Vol. 10, 1979, pp. 483-493.

16 Hinton, E., Salonen, E. M., and Bicanic, N., "A Study of Locking Phenomena in Isoparametric Elements," Third MAFELAP Conference, Brunel University, Oxbridge, 1978.

17 Horrignoe, G., "Finite Element Instability Analysis of Free-Form Shells," Report 77-2, Division of Structural Mechanics, Norwegian Institute of Technology, University of Trondheim, Norway, May 1977.

18 Hughes, T. J. R., "Generalization of Selective Integration Procedures to Anisotropic and Nonlinear Media," *International Journal of Numerical Methods in Engineering*, Vol. 15, 1980, pp. 1413-1418.

19 Hughes, T. J. R., "Recent Developments in Computer Methods for Structural Analysis," *Nuclear Engineering and Design*, Vol. 57, No. 2, 1980, pp. 427-439.

20 Hughes, T. J. R., and Cohen, M., "The 'Heterosis' Finite Element for Plate Bending," *Computers and Structures*, Vol. 9, 1978, pp. 445-450.

21 Hughes, T. J. R., and Cohen, M., "The 'Heterosis' Family of Plate Finite Elements," *Proceedings of the ASCE Electronic Computations Conference*, St. Louis, Mo., August 6-8, 1979.

22 Hughes, T. J. R., Cohen, M., and Haroun, M., "Reduced and Selective Integration Techniques in the Finite Element Analysis of Plates," *Nuclear Engineering and Design*, Vol. 46, 1978, pp. 203-222.

23 Hughes, T. J. R., and Liu, W. K., "Nonlinear Finite Element Analysis of Shells: Part I. Three-Dimensional Shells," *Computer Methods in Applied Mechanics and Engineering*, to appear.

24 Hughes, T. J. R., and Liu, W. K., "Nonlinear Finite Element Analysis of Shells: Part II. Two-Dimensional Shells," *Computer Methods in Applied Mechanics and Engineering*, to appear.

25 Hughes, T. J. R., Liu, W. K., and Levit, I., "Nonlinear Dynamic Finite Element Analysis of Shells," *Proceedings of the Europe-U.S. Workshop on Finite Element Methods in Structural Mechanics*, Bochum, West Germany, July 28-31, 1980.

26 Hughes, T. J. R., Taylor, R. L., and Kanoknukulchai, W., "A Simple and Efficient Element for Plate Bending," *International Journal for Numerical Methods in Engineering*, Vol. 11, No. 10, 1977, pp. 1529-1543.

27 Irons, B. M., "The Semiloof Shell Element," *Finite Elements for Thin Shells and Curved Members*, eds., Ashwell, D. G., and Gallagher, R. H., John Wiley, New York, 1976, Chapter 11, pp. 197-222.

28 Kanoknukulchai, W., "A Large Deformation Formulation for Shell Analysis by the Finite Element Method," PhD Thesis, University of California, Berkeley, Nov. 1978.

29 Kanoknukulchai, W., "A Simple and Efficient Finite Element for General Shell Analysis," *International Journal for Numerical Methods in Engineering*, Vol. 14, 1979, pp. 179-200.

30 Kosloff, D., and Frazier, G., "Treatment of Hourglass Patterns in Low Order Finite Element Codes," *Numerical and Analytical Methods in Geomechanics*, Vol. 2, 1978, pp. 57-72.

31 MacNeal, R. H., "A Simple Quadrilateral Shell Element," *Computers and Structures*, Vol. 8, 1978, pp. 175-183.

32 Malkus, D. S., "Finite Element Analysis of Incompressible Solids," PhD Dissertation, Boston University, Boston, Mass., 1975.

33 Malkus, D. S., "A Finite Element Displacement Model Valid for any Value of the Compressibility," *International Journal of Solids and Structures*, Vol. 12, 1976, pp. 731-738.

34 Malkus, D. S. and Hughes, T. J. R., "Mixed Finite Element Methods—Reduced and Selective Integration Techniques: A Unification of Concepts," *Computer Methods in Applied Mechanics and Engineering*, Vol. 15, No. 1, 1978, pp. 63-81.

35 Mindlin, R. D., "Influence of Rotatory Inertia and Shear on Flexural Motions of Isotropic, Elastic Plates," *ASME JOURNAL OF APPLIED MECHANICS*, Vol. 18, 1951, pp. 31-38.

36 Nagtegaal, J. C., Parks, D. M., and Rice, J. R., "On Numerically Accurate Finite Element Solutions in the Fully Plastic Range," *Computer Methods in Applied Mechanics and Engineering*, Vol. 4, 1974, pp. 153-178.

37 Noor, A. K., and Peters, J. M., "Mixed Models and Reduced/Selective Integration Displacement Models for Nonlinear Analysis of Curved Beams," *International Journal for Numerical Methods in Engineering*, to appear.

38 Oden, J. T., Kikuchi, N., and Song, Y. J., "Reduced Integration and Exterior Penalty Methods for Finite Element Approximations of Contact Problems in Incompressible Elasticity," TICOM 80-2, Texas Institute for Computational Mechanics, Univ. of Texas, Austin, 1980; submitted for review to *SIAM Journal of Numerical Analysis*.

39 Parisch, H., "A Critical Survey of the 9-Node Degenerated Shell Element With Special Emphasis on Thin Shell Application and Reduced Integration," *Computer Methods in Applied Mechanics and Engineering*, Vol. 20, 1979, pp. 323-350.

40 Pawsey, S. E., and Clough, R. W., "Improved Numerical Integration of Thick Shell Finite Elements," *International Journal for Numerical Methods in Engineering*, Vol. 3, 1971, pp. 545-586.

41 Pica, A., and Hinton, E., "Efficient Transient Dynamic Plate Bending Analysis With Mindlin Elements," *Earthquake Engineering and Structural Dynamics*, to appear.

42 Pugh, E. D. L., Hinton, E., and Zienkiewicz, O. C., "A Study of Quadrilateral Plate Bending Elements With 'Reduced' Integration," *International Journal for Numerical Methods in Engineering*, Vol. 12, No. 7, 1978, pp. 1059-1079.

43 Ramm, E., "A Plate/Shell Element for Large Deflection and Rotations," *Formulations and Computational Algorithms in Finite Element Analysis*, Bathe, K. J., Oden, J. T., and Wunderlich, W., eds., M.I.T. Press, Cambridge, Mass., 1977.

44 Reddy, J. N., "A Comparison of Closed-Form and Finite-Element Solutions of Thick, Laminated, Anisotropic Rectangular Plates," Report OU-AMNE-79-19, University of Oklahoma, Norman, Okla., Dec. 1979.

45 Robinson, J., "LORA—An Accurate Four Node Stress Plate Bending Element," *International Journal of Numerical Methods in Engineering*, Vol. 14, No. 2, 1979, pp. 296-306.

46 Rossow, M., "Efficient C° Finite-Element Solution of Simply Supported Plates of Polygonal Shape," *ASME JOURNAL OF APPLIED MECHANICS*, Vol. 44, 1977, pp. 347-349.

47 Sander, G., "Application of the Dual Analysis Principle," *Proceedings of the IUTAM Symposium*, Liege, Belgium, 1971, pp. 167-207.

48 Song, Y. J., Oden, J. T., and Kikuchi, N., "Discrete LBB Condition for RIP Finite Element Methods," TICOM 80-7, Texas Institute for Computational Mechanics, University of Texas, Austin, 1980, submitted for review to *SIAM Journal of Numerical Analysis*.

49 Spilker, R. L. and Munir, N. I., "The Hybrid-Stress Model for Thin Plates," *International Journal for Numerical Methods in Engineering*, Vol. 15, No. 8, Aug. 1980, pp. 1239-1260.

50 Spilker, R. L., and Munir, N. I., "A Serendipity Cubic-Displacement Hybrid-Stress Element for Thin and Moderately Thick Plates," *International Journal for Numerical Methods in Engineering*, Vol. 15, No. 8, Aug. 1980, pp. 1261-1278.

51 Spilker, R. L., and Munir, N. I., "A Hybrid-Stress Quadratic Serendipity Displacement Mindlin Plate Bending Element," *Computers and Structures*, to appear.

52 Taylor, R. L., "Finite Elements for General Shell Analysis," Preprints of the 5th International Seminar on Computational Aspects of the Finite Element Method, Berlin (West), Germany, August 20-21, 1979.

53 Zienkiewicz, O. C., *The Finite-Element Method*, 3rd ed., McGraw-Hill, London, 1977.

54 Zienkiewicz, O. C., et al., "A Simple Element for Axisymmetric Shells With Shear Deformation," *International Journal for Numerical Methods in Engineering*, Vol. 11, 1977, pp. 1545-1558.

55 Zienkiewicz, O. C., and Hinton, E., "Reduced Integration, Function Smoothing and Nonconformity in Finite Element Analysis," *Journal of The Franklin Institute*, Vol. 302, 1976, pp. 443-461.

56 Zienkiewicz, O. C., Taylor, R. L., and Too, J. M., "Reduced Integration Technique in General Analysis of Plates and Shells," *International Journal for Numerical Methods in Engineering*, Vol. 3, 1971, pp. 275-290.